Int. J. Solids Structures, 1971, Vol. 7, pp. 805 to 823. Pergamon Press. Printed in Great Britain

THE USE OF FINITE ELEMENT MID-INCREMENT STIFFNESS MATRICES IN THE POST-BUCKLING ANALYSIS OF IMPERFECT STRUCTURES

T. M. ROBERTS and D. G. ASHWELL

Department of Civil and Structural Engineering, University College, Cardiff, U.K.

Abstract—The advantage of using a linearized mid-increment stiffness matrix in the finite element incremental analysis of nonlinear structures is demonstrated. The method is applied to the post-buckling analysis of an imperfect strut and plate. Features of the paper are a clear presentation of the incremental process, the use of Marguerre's shallow shell theory to avoid transformations between local and global axes, and the calculation of stresses in the post-buckled state. The computational similarity of the incremental and Newton–Raphson iterative processes is pointed out.

1. INTRODUCTION

THE earliest work on the finite element analysis of the geometrically nonlinear behaviour of structures is that of Turner *et al.* [1]. They described the use of linear increments, with an "initial stress" or "geometric" stiffness matrix recalculated before each increment. An alternative method was used by Oden and Sato [2] who solved the nonlinear equations by the Newton–Raphson iterative procedure (see also Zarghamee and Shah [3] and Walker [4]). Martin [5] gives an account of work up to 1965, which was mainly concerned with beam elements and Mallett and Marcal [6] summarize later work. More recently attention has been directed to the large deflection of plates (Kawai and Yoshimura [7], Brebbia and Connor [8], Murray and Wilson [9]).

The solution of such problems is very expensive in both computer time and storage. The present paper describes the use of mid-increment stiffness matrices which greatly reduce the number of increments required to achieve a given accuracy. This is first demonstrated by considering the large deflection of a laterally-loaded square plate. The method is then applied to the postbuckling behaviour of an imperfect strut and an imperfect simply-supported square plate with in-plane compression.

A slender strut is found to fail at a load close to the theoretical Euler critical load, but this is not true of plates in compression. Lateral constraints at the longitudinal edges can lead to a redistribution of the membrane compression, and such panels are able to withstand loads several times greater than the theoretical buckling load. Levy [12] gives an exact (Fourier series) solution for a simply-supported plate with longitudinal edges free to move but constrained to remain straight. Hu *et al.* [13] extend the solution to include imperfections and show that their solution converges to Levy's for loads of two or three times the critical load.

Schmit *et al.* [11] have tackled the problem using finite elements. They iterate to a minimum of potential energy, using a fully compatible rectangular element with 48 degrees of freedom. Murray and Wilson [10] also use an iterative method and triangular elements that

require transformation from local to global axes. In the present paper a rectangular shell element is used, which having only 20 degrees of freedom is much simpler than that used by Schmit *et al.*, and being treated within the framework of shallow shell theory does not require transformation of axes. The method of incrementing displacements is used, with a linearized mid-increment stiffness matrix calculated for each increment of displacement. Results obtained agree well with known analytical solutions for both imperfect struts and plates. Stresses are calculated as well as deflections, and a feature of the paper is the very simple presentation of the derivation of the incremental stiffness matrix.

A similar type of shallow element for the large deflections of plates, has been used by Brebbia and Connor [8].

The nonlinear behaviour of plates was considered by von Karman [14], with the assumption that although the deflections w, from the initial x, y plane, are sufficient to cause significant membrane stress resultants—and therefore to invalidate linear plate theory —slopes $\partial w/\partial x$, $\partial w/\partial y$ remain much less than unity. Von Karman's pair of simultaneous nonlinear differential equations for w and the membrane stress function F were extended by Marguerre [15] to the case of plates which when unstressed have $w = w_0 \neq 0$, i.e. to the case of shallow shells. (See Reissner [16] for an account of shallow shell theory.) In the present paper we do not employ Marguerre's differential equations, but use the corresponding potential energy function to derive the linearized incremental stiffness matrix for a rectangular element (see Appendix 1).

2. THEORY

Consider a structure in equilibrium under the action of forces P_i, the deflected form being defined by a finite number of corresponding displacements q_i.

Then Castigliano's theorem states

$$\frac{\partial U}{\partial q_i} = P_i \tag{1}$$

where U is the strain energy of the structure expressed as a function of the q_i. Let Δ denote increments in these quantities so that the structure remains in equilibrium. Then

$$\frac{\partial(U+\Delta U)}{\partial(q_i+\Delta q_i)} = P_i+\Delta P_i. \tag{2}$$

If U and q_i are regarded as constant, only ΔU and Δq_i varying,

$$\frac{\partial(U+\Delta U)}{\partial(q_i+\Delta q_i)} = \frac{\partial \Delta U}{\partial \Delta q_i}.$$

Therefore

$$\frac{\partial \Delta U}{\partial \Delta q_i} = P_i+\Delta P_i. \tag{3}$$

Equation (3) provides a basis for what is referred to in the literature as the incremental method. We now derive the incremental stiffness matrix for a curved beam element. The extension to shells follows along similar lines (see Appendix 1) but involves considerable work.

Consider the element shown in Fig. 1, with cross section area A, second moment of area I and Young's modulus E. w_0 defines the initial shape, and w and u the deformed shape, where w_0, w and u may be expressed as linear functions of the displacements at nodes A and B. On the assumption that $(dw/dx)^2$ can be neglected compared with unity we can express the strain energy of the element as follows:

$$U = \frac{EI}{2}\int_0^a \left[\frac{d^2w}{dx^2} - \frac{d^2w_0}{dx^2}\right]^2 dx + \frac{EA}{2}\int_0^a \left[\frac{du}{dx} + \frac{1}{2}\left(\frac{dw}{dx}\right)^2 - \frac{1}{2}\left(\frac{dw_0}{dx}\right)^2\right]^2 dx \tag{4}$$

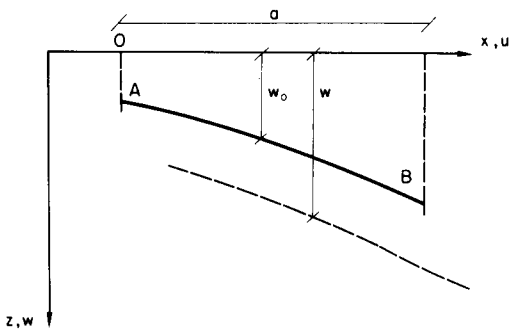

FIG. 1. Shallow curved beam element.

where the first term represents the strain energy of bending and the second the axial strain energy. Let Δ denote increments in the above quantities and suffices x, xx denote differentiation.

$$U + \Delta U = \frac{EI}{2}\int_0^a [w_{xx} + \Delta w_{xx} - w_{0,xx}]^2 dx + \frac{EA}{2}\int_0^a [u_x + \Delta u_x + \tfrac{1}{2}(w_x + \Delta w_x)^2 - \tfrac{1}{2}w_{0,x}^2]^2\, dx \tag{5}$$

If $\delta\Delta q_i$ represent small variations in the Δq_i equation (3) can be rewritten

$$\delta\Delta q_i \frac{\partial \Delta U}{\partial \Delta q_i} = (P_i + \Delta P_i)\,\delta\Delta q_i \tag{6}$$

where repeated suffixes imply summation. ΔU will contain terms which are linear functions of Δq_i, quadratic functions of Δq_i and higher order functions of Δq_i. Differentiation of the linear terms gives rise to constants which must be equal to P_i, while differentiation of the quadratic terms leads to linear functions of Δq_i which are equated to ΔP_i. Higher order terms in Δq_i are neglected to make the problem incrementally linear. Hence, on substituting ΔU from equations (5) and (4) into equation (6), cancelling terms equivalent to P_i and

neglecting terms of third and higher order in Δq_i we have

$$\delta\Delta q_i \Delta P_i = \frac{EI}{2}\int_0^a 2\Delta w_{xx}\,\delta\Delta w_{xx}\,dx + \frac{EA}{2}\int_0^a [2\Delta u_x\,\delta\Delta u_x + 2u_x\Delta w_x\,\delta\Delta w_x + 2w_x(\Delta u_x\,\delta\Delta w_x + \Delta w_x\,\delta\Delta u_x) + 3w_x^2\Delta w_x\,\delta\Delta w_x - w_{0,x}^2\Delta w_x\,\delta\Delta w_x]\,dx. \tag{7}$$

Since Δw_{xx} is a function of the nodal displacements Δq_i, $\delta\Delta w_{xx}$ is a function of $\delta\Delta q_i$. Equation (7) can now be conveniently expressed in matrix form as follows:

$$\{\delta\Delta q\}^T\{\Delta P\} = \int_0^a [\delta\Delta w_{xx}, \delta\Delta u_x]\left[\begin{array}{c|c} EI & \\ \hline & EA \end{array}\right]\left[\begin{array}{c} \Delta w_{xx} \\ \Delta u_x \end{array}\right]dx + EA\int_0^a [\delta\Delta w_x, \delta\Delta u_x]\left[\begin{array}{c|c} \frac{3}{2}w_x^2 - \frac{1}{2}w_{0,x}^2 + u_x & w_x \\ \hline w_x & \end{array}\right]\left[\begin{array}{c} \Delta w_x \\ \Delta u_x \end{array}\right]dx. \tag{8}$$

All that remains is to relate the displacement functions w, u to the nodal displacements q_i. This is achieved by choosing suitable polynomial shape functions as follows:

$$w = [1, x, x^2, x^3, 0, 0, 0, 0]\{\alpha\}$$
$$u = [0, 0, 0, 0, 1, x, x^2, x^3]\{\alpha\}.$$

Let the nodal displacements defining w be

$$w_A, \theta_A \equiv \left.\frac{dw}{dx}\right|_A, \qquad w_B, \qquad \theta_B$$

and those defining u be u_A, $u_{A,x}$, u_B, $u_{B,x}$ (Fig. 1). Here $u_{A,x}$ means the value of du/dx at A. Then taking the origin of co-ordinates at 0 in Fig. 1

$$w_B = [1, a, a^2, a^3, 0, 0, 0, 0]\{\alpha\}.$$

Treating all the other nodal displacements in a similar way we arrive at the matrix expression

$$\begin{bmatrix} w_A \\ \theta_A \\ u_A \\ u_{A,x} \\ w_B \\ \theta_B \\ u_B \\ u_{B,x} \end{bmatrix} = [A]\{\alpha\} = \{q\}. \tag{9}$$

$\{\alpha\}$ are referred to as polynomial coefficients and $[A]$ is an (8, 8) matrix relating polynomial coefficients to nodal displacements.

From equation (9)

$$\{\alpha\} = [A]^{-1}\{q\}. \tag{10}$$

Now

$$w_{xx} = [0, 0, 2, 6x, 0, 0, 0, 0]\{\alpha\}$$

and we can express

$$\begin{bmatrix} w_{xx} \\ u_x \end{bmatrix} = [S_1]\{\alpha\}; \qquad \begin{bmatrix} w_x \\ u_x \end{bmatrix} = [S_2]\{\alpha\} \tag{11}$$

where $[S_1]$ and $[S_2]$ are (2, 8) matrices obtained by differentiation of the displacement functions.

Also let

$$[K_1] = \left[\begin{array}{c|c} EI & \\ \hline & EA \end{array}\right]; \qquad [K_2] = \left[\begin{array}{c|c} \frac{3}{2}w_x^2 - \frac{1}{2}w_{0,x}^2 + u_x & w_x \\ \hline w_x & \end{array}\right]. \tag{12}$$

Substituting equations (10)–(12) into equation (8) we have

$$\{\delta\Delta q\}^T\{\Delta P\} = \{\delta\Delta q\}^T[A]^{-1T}\int_0^a [S_1]^T[K_1][S_1]\,dx[A]^{-1}\{\Delta q\}$$

$$+\{\delta\Delta q\}^T[A]^{-1}\int_0^a [S_2]^T[K_2][S_2]\,dx[A]^{-1}\{\Delta q\}. \tag{13}$$

Since this equation holds for any $\{\delta\Delta q\}$ it follows that

$$\{\Delta P\} = [[K_{\text{lin}}]+[K_G]]\{\Delta q\}$$

where

$$[K_{\text{lin}}] = [A]^{-1T}\int_0^a [S_1]^T[K_1][S_1]\,dx[A]^{-1}$$

$$[K_G] = [A]^{-1T}\int_0^a [S_2]^T[K_2][S_2]\,dx[A]^{-1}.$$

$[K_G]$ is often referred to as the geometric or initial stress stiffness matrix.

Combining $[K_{\text{lin}}+K_G]$ to form the incremental stiffness matrix $[K_{\text{inc}}]$

$$\{\Delta P\} = [K_{\text{inc}}]\{\Delta q\}. \tag{14}$$

Equation (14) relates the increase in nodal forces $\{\Delta P\}$ to the increase in nodal displacements $\{\Delta q\}$.

It will be noticed that $[K_G]$ necessitates the integration of functions such as $x^2w_x^2$ over the length of the element. For the case under consideration this does not prove a severe obstacle. However, in the case of a shell element, w contains twelve terms so that numerical integration is advisable.

The individual element stiffness matrices can be assembled to give the incremental stiffness matrix for the complete structure.

3. SOLUTION OF EQUATIONS

The solution of any problem by the finite element method eventually reduces to the solution of a set of simultaneous equations. For the incremental method, since $[K_G]$ depends upon the deformed shape prior to additional disturbances, the incremental stiffness matrix has to be reformed and the equations solved at each step. It is very important therefore, when dealing with large numbers of equations, as in the large deflection of plates and shells, to optimize the solution routine.

The method adopted in the present work was a half band single term elimination process (Brooks and Brotton [17]). Two further refinements were introduced, incrementing displacements rather than loads (Argyris [18]) and the use of what we shall call the mid-increment stiffness. These have the following advantages.

(a) No prior knowledge of the load–deflection curve is required, only the magnitudes of the deflections which are to be considered, e.g. in the nonlinear analysis of plates we may require a central deflection of two to three times the plate thickness.

(b) The solution does not fail at a horizontal tangent on the load–deflection curve, e.g. at snapping of a shallow arch.

(c) Use of the mid-increment stiffness, derived as follows, reduces the number of incremental steps required for any problem. At a particular stage of the incremental process the deformed shape, and hence the incremental stiffness, depends on $\{q\}_n$. To arrive at the next equilibrium position on the curve

$$\{q\}_n + \{\Delta q\}_{n+1} = \{q\}_{n+1}$$

it would be desirable to derive the incremental stiffness from the mean value of these displacements

$$\{q\}_n + \tfrac{1}{2}\{\Delta q\}_{n+1}.$$

However, $\{\Delta q\}_{n+1}$ is not known, but an approximation can be obtained by assuming that $\{\Delta q\}_{n+1}$ is not very different from $\{\Delta q\}_n$. The incremental stiffness is then derived from displacements $\{q\}_n + \frac{1}{2}\{\Delta q\}_n$. Solutions of the large deflections of plates subjected to lateral loading show that this technique can at least halve the number of increments required to attain a particular accuracy.

The procedure for incrementing displacements can be illustrated briefly as follows. Suppose we wish to solve the equations

$$\begin{bmatrix} a_1 & a_2 & a_3 \\ b_1 & b_2 & b_3 \\ c_1 & c_2 & c_3 \end{bmatrix} \begin{bmatrix} q_1 \\ q_2 \\ q_3 \end{bmatrix} = \begin{bmatrix} P_1 \\ P_2 \\ P_3 \end{bmatrix} \tag{15}$$

subject to the condition that $q_2 = Q$. For proportional loading the load vector can be replaced by $P_1 = r_1\gamma$, $P_2 = r_2\gamma$, $P_3 = r_3\gamma$ where the r's are the ratios of the magnitudes of the applied loads and γ is a variable which defines their magnitudes. Expanding equation (15)

$$\begin{bmatrix} a_1 & 0 & a_3 \\ b_1 & 0 & b_3 \\ c_1 & 0 & c_3 \end{bmatrix} \begin{bmatrix} q_1 \\ 0 \\ q_3 \end{bmatrix} + \begin{bmatrix} a_2 \\ b_2 \\ c_2 \end{bmatrix} \times Q = \begin{bmatrix} r_1 \\ r_2 \\ r_3 \end{bmatrix} \times \gamma .$$

Rearranging

$$\begin{bmatrix} a_1 & -r_1 & a_3 \\ b_1 & -r_2 & b_3 \\ c_1 & -r_3 & c_3 \end{bmatrix} \begin{bmatrix} q_1 \\ \gamma \\ q_3 \end{bmatrix} = \begin{bmatrix} a_2 \\ b_2 \\ c_2 \end{bmatrix}^{\times -Q} . \tag{16}$$

Equation (16) can be solved for q_1, γ, q_3 and the magnitudes of the applied loads determined.

The manipulations necessary to combine this with the half band solution will not be discussed as this would necessitate a full explanation of the banded solution itself.

4. LATERALLY LOADED SQUARE PLATE

To demonstrate the use of the mid-increment stiffness, a clamped square plate was considered (Fig. 2) with side a, thickness h, Young's modulus E and uniform lateral pressure p. Poisson's ratio was taken as 0·3. The quarter plate was divided into 16 square elements, with the shape functions given in Appendix 1. The central displacement w_c was incremented within the range $0 < w_c < 2h$.

When the final deflection $w_c = 2h$ had been reached, the solution was refined by the Newton–Raphson iterative process (Hilderbrand [19]). This process can conveniently be combined with the incremental process because the Jacobian matrix which must be recalculated for each iteration of the Newton–Raphson process is identical with the incremental stiffness matrix which must be recalculated for each increment (see Appendix 2). Solutions were considered to have converged when

$$\frac{1}{n}\sum_{i=1}^{n}\left(\frac{\Delta q_i}{q_i+\Delta q_i}\right)^2 < 0{\cdot}0001$$

where n is the number of nodal displacements ($n = 125$). Results are shown on Fig. 2, together with a Fourier series solution by Levy [20].

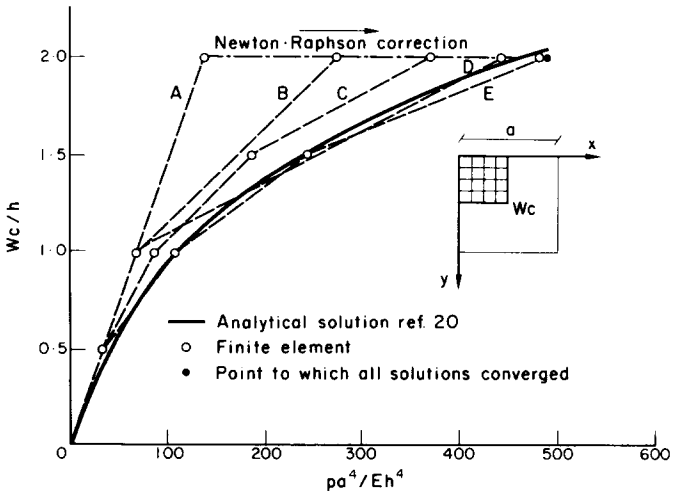

FIG. 2. Comparison of incremental solutions including Newton–Raphson correction.

Five solutions were performed, all converging to the final point:
(a) single increment followed by 3 iterations;
(b) 2 normal increments followed by 3 iterations;
(c) 4 normal increments followed by 2 iterations;
(d) 2 mid-increments followed by 2 iterations;
(e) 4 mid-increments followed by 2 iterations.

The errors in the final values of the load obtained by the incremental processes, i.e. before the Newton–Raphson iterations were: (a) 72 per cent; (b) 44 per cent; (c) 25 per cent; (d) 10 per cent; (e) 1 per cent. Comparison of (b) with (d) and (c) with (e) shows the great advantage in using the mid-increment stiffness matrices.

The solutions also show the usefulness of the iterative process when combined with a coarse incremental solution. Two iterations were required in solution (e) because the first iteration, though very close to the convergence limit, was just outside it; this was not so for solutions (c) and (d).

Times required on the Atlas computer at Harwell were approximately 1 min for each increment and 2 min for each iteration.

5. IMPERFECT STRUT

In the remainder of this paper results are given for two post-buckling problems for imperfect structures, obtained by incrementing displacements. The first is the strut shown in Fig. 3, having a small initial bow $w_0 = c \sin(\pi x/l)$. This problem was chosen since an analytical solution is readily obtained. Eight curved beam elements were used for the complete strut, and two increment sizes (using mid-increment stiffness). The results are shown in Figs. 4 and 5, for $l = 40$ in., $c = 0{\cdot}1$ in., area of cross-section $= 1{\cdot}225$ in.^{2}, second moment of area $= 0{\cdot}153125$ in.^{4}, $E = 10^7$ lbf in.$^{-2}$.

6. IMPERFECT PLATE IN COMPRESSION

To test the applicability of the finite element solution to the postbuckling behaviour of plates we consider the case of a simply-supported square plate subject to membrane stresses in the x-direction (Fig. 6). This problem has been solved using Fourier series by Levy [12] for a perfectly flat plate, and by Hu *et al.* [13] for a plate with an initial deviation from flatness defined by

$$w_0 = c \operatorname{cin}(\pi x/a) \sin(\pi y/a).$$

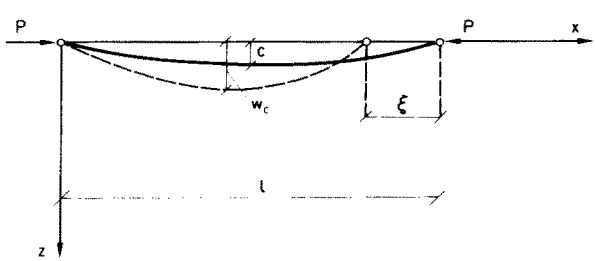

FIG. 3. Initially imperfect strut.

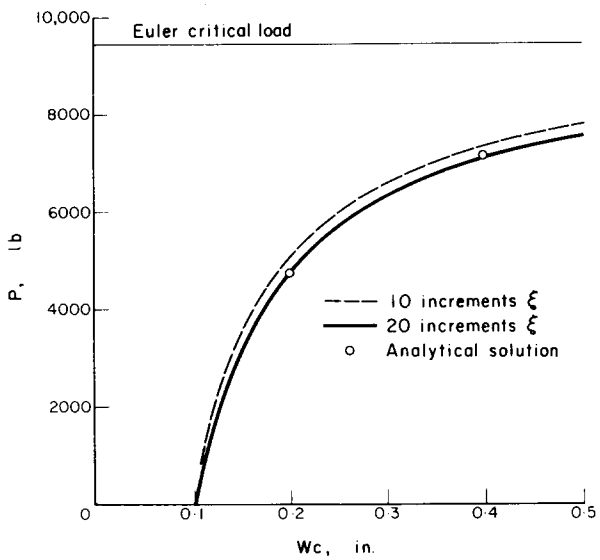

FIG. 4. Variation of central deflection with axial load for an imperfect strut.

The in-plane boundary conditions are such that all edges of the plate remain straight and the average membrane stress $\bar{\sigma}_y$ along AM and NL is zero. The total compressive force in the x-direction is $\bar{\sigma}_x ah$.

For the finite element analysis, Poisson's ratio was taken as 0·3 as against 0·316 for the analytical solutions. A trial run with $\gamma = 0{\cdot}316$ showed that the variation in results due to this small discrepancy was negligible. Sixteen elements (see Appendix 1) were used on a quarter of the plate and displacement increments made at point C in the x-direction. The edges were constrained to remain straight by introducing stiffeners such that any relative

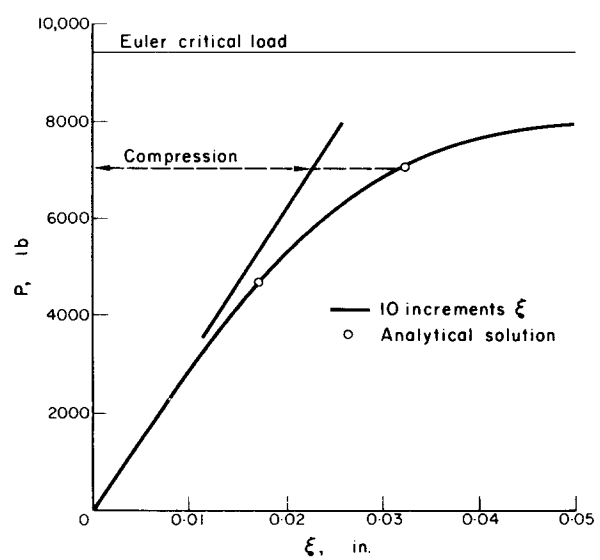

FIG. 5. Variation of end displacement with axial load for an imperfect strut.

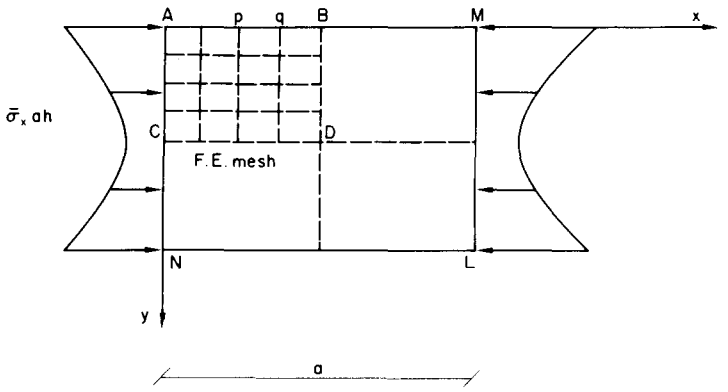

FIG. 6. Initially imperfect plate.

in-plane displacement of points p, q say, normal to AM would result in a considerable increase in the strain energy of the structure. It was found that if the stiffeners were made too rigid (achieved by adding large numbers to appropriate elements of the stiffness matrix) the solution became ill-conditioned. Because of this the present solution contains discrepancies of approximately 2 per cent in the in-plane displacements of B and C relative to the corners of the plate. The introduction of stiffeners also permitted the non-uniform membrane stress σ_x to be applied by means of equal point loads along sides AN and ML, so that the ratios r_i in equation (16) were known. The initial deviation from flatness considered was the maximum given in [13] i.e. $c = 0{\cdot}1h$. It is important to notice that the present approach requires that $c \neq 0$; otherwise there would be no interaction between bending and membrane stresses, and a stability analysis would have to be carried out to give an initial shape from which to begin the incremental analysis.

Figure 7 shows the variation of central deflection with the average compressive stress $\bar{\sigma}_x$. σ_{cr} is the critical stress for a flat plate with the same boundary conditions. Figure 8 shows that the effective width ratio b_e/b defined as the actual load carried by the plate divided by the load the plate would have carried for the same edge displacement had it remained perfectly flat, decreases as $\bar{\sigma}_x$ increases.

Since [13] gives results only up to $\bar{\sigma}_x = 2\sigma_{cr}$, finite element results for higher values of $\bar{\sigma}_x$ are compared in Figs. 9 and 10 with Levy's solution for a perfectly flat plate. Also included on Fig. 10 is the approximate solution of Marguerre [21], $b_e/b = \frac{1}{2}(1 + 1/n)$ where n is the actual edge displacement over the critical edge displacement.

To investigate the distribution of stress throughout the plate, bending and membrane stresses were calculated at the centre of each element. This procedure was adopted for two reasons:

(a) The displacement functions chosen do not give continuity of stress along the element boundaries or at the nodes, therefore some form of smoothing process is required.

(b) Experience has shown that calculating membrane stresses at built-in edges, e.g. in the large deflections of a built-in plate, leads to erroneous results, whereas the stresses calculated at the centre of each element are in good agreement with analytical solutions. This is probably due to the choice of simple shape functions to represent the in-plane displacements.

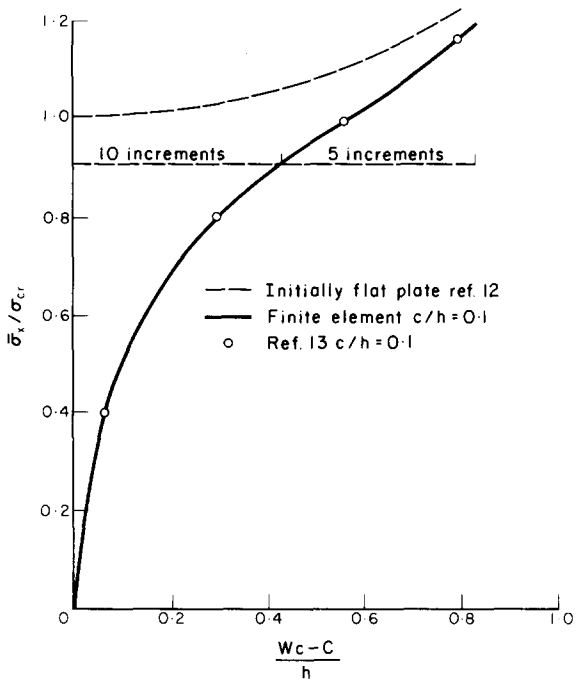

FIG. 7. Variation of central deflection with average compressive stress.

Figures 11 and 12 give the distribution of membrane stresses for two values of $\bar{\sigma}_x a^2/Eh^2$ which are indicated on the curves. These two values, 14·1 and 8·95 correspond to approximately 7 and 4 times the critical edge-displacement. The values from [12] calculated at the corners of the elements, i.e. points A, B, C, D are included for comparison since an overall

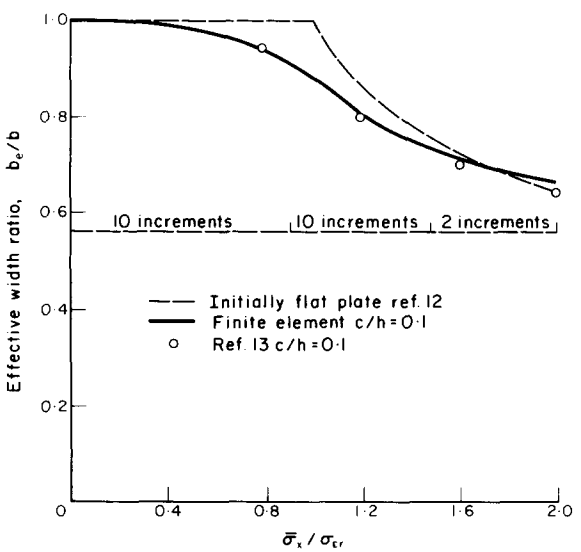

FIG. 8. Variation of effective width ratio with average compressive stress.

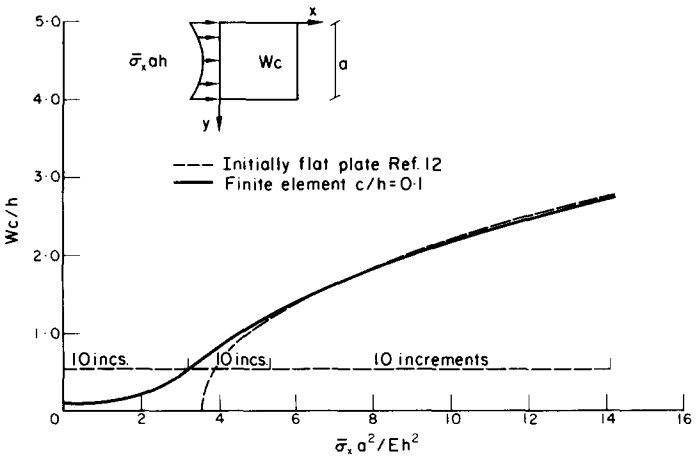

FIG. 9. Variation of central deflection with average compressive stress.

plot showed that the membrane stresses were not varying very steeply towards the edges of the elements.

Figure 13 shows similar curves for the extreme fibre bending stress σ_{xb} along *RS*. Here the agreement with [12] calculated at the corners is not so good but an overall plot of the bending moments showed that for $\bar{\sigma}a^2/Eh^2 = 14{\cdot}1$ they were varying quite steeply towards the line *BD*. Also included on Fig. 13 are values of σ_{xb} along *BD* obtained by plotting values at the centre of the elements, along lines *tt*, and drawing smooth curves through them. These show much better agreement with [12].

Where it is thought useful the number of increments used in the solution are indicated on the curves.

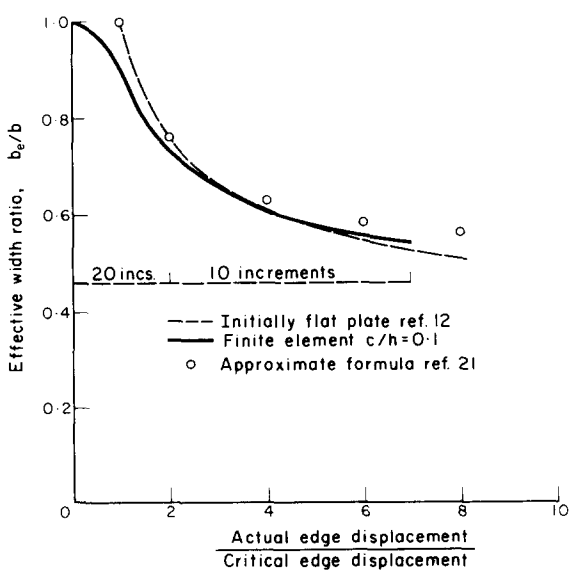

FIG. 10. Effective width ratio.

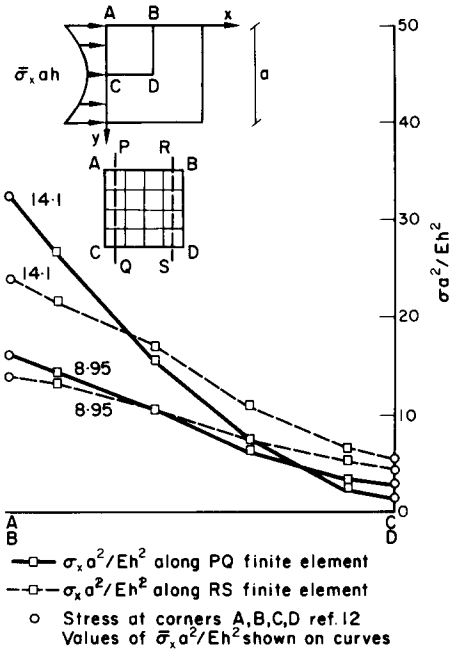

FIG. 11. Membrane stresses.

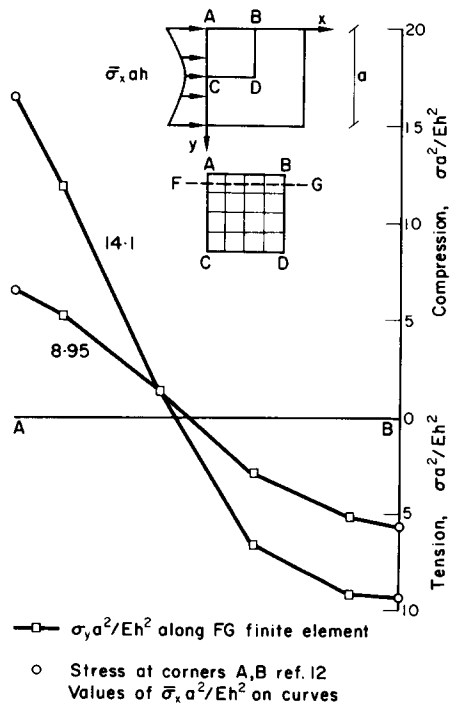

FIG. 12. Membrane stresses.

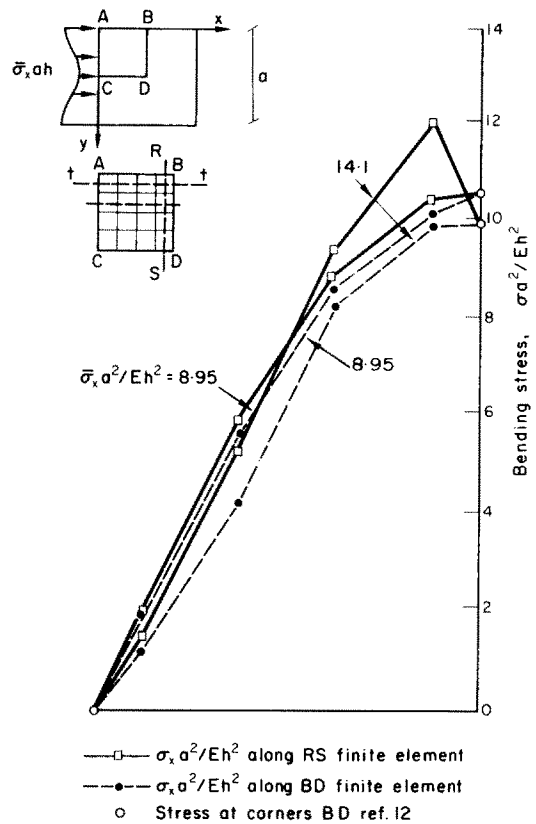

FIG. 13. Bending stresses.

7. DISCUSSION

The main restriction on the use of finite element techniques is the capability of the computer to deal with large sets of simultaneous equations quickly and efficiently. Due to the highly nonlinear behaviour of plates near their critical load, as many as thirty increments were used to obtain the results for the post-buckling problem, which meant assembling and solving a set of 125 degrees of freedom, thirty times. However, satisfactory results could have been obtained using less than half this number of increments (checked using Newton–Raphson iteration). The time for one increment on the Atlas computer at Harwell was approximately 1 min resulting in a considerable cost for the complete solution. When such a large number of increments is required it is more economical to solve the set of nonlinear algebraic equations resulting from equation (1) when U is expressed in terms of nonlinear strain displacement relationships. One such method of solution is the Newton–Raphson method which was used in Section 4.

The capability of the finite element method to deal with almost any type of boundary conditions, anisotropy, material imperfections and plasticity should be taken into consideration when discussing the economics of the method.

REFERENCES

[1] M. J. TURNER, E. H. DILL, H. C. MARTIN and R. J. MELOSH, Large deflection of structures subjected to heating and external loads. *J. aeronaut. Sci.* **27**, 97–106 (1960).
[2] J. T. ODEN and T. SATO, Finite strains and displacements of elastic membranes by the finite element method. *Int. J. Solids Struct.* **3**, 471–488 (1967).
[3] M. S. ZARGHAMEE and H. M. SHAH, Stability of space frames. *Proc. Am. Soc. civ. Engrs* **94**, EM2, 371–384 (1968).
[4] A. C. WALKER, A nonlinear finite element analysis of shallow circular arches. *Int. J. Solids Struct.* **5**, 97–107 (1969).
[5] H. C. MARTIN, On the derivation of stiffness matrices for the analysis of large deflections and stability problems. *Proc. Conf. Matrix Methods in Structural Mechanics.* Air Force Inst. of Tech., Wright Patterson A.F.B. (1965).
[6] R. H. MALLETT and P. V. MARCAL, Finite element analysis of nonlinear structures. *Proc. Am. Soc. civ. Engrs* **94**, ST9, 2081–2105 (1968).
[7] T. KAWAI and N. YOSHIMURA, Analysis of large deflection of plates by the finite element method. *Int. J. Numerical Meth. Engng* **1**, 123–133 (1969).
[8] C. BREBBIA and J. CONNOR, Geometrically nonlinear finite element analysis. *Proc. Am. Soc. civ. Engrs* **95**, EM2, 463–483 (1969).
[9] D. W. MURRAY and E. L. WILSON, Finite element large deflection of plates. *Proc. Am. Soc. civ. Engrs* **95**, EM1, 143–165 (1969).
[10] D. W. MURRAY and E. L. WILSON, Finite element postbuckling analysis of thin elastic plates. *AIAA Jnl* **7**, 1915–1920 (1969).
[11] L. A. SCHMIT, F. K. BOGNER and R. L. FOX, Finite deflection analysis using plate and cylindrical shell discrete elements. *AIAA Jnl* **6**, 781–791 (1968).
[12] S. LEVY, Bending of rectangular plates with large deflections—NACA TN.846 (1942).
[13] P. C. HU, E. E. LUNDQUIST and S. B. BATDORF, Effect of small deviations from flatness on effective width and buckling of plates in compression—NACA. TN. 1124 (1946).
[14] TH. VON KARMAN, *Encyklopadie der Mathematischen Wissenschaften*, Vol. 4, p. 349. Teubner (1910).
[15] K. MARGUERRE, Zur theorie der gekrummten platte grosser formanderung, *Proc. 5th Int. Cong. Appl. Mech. Cambridge, Mass.* (1938).
[16] E. REISSNER, On some aspects of the theory of thin elastic shells. *J. Boston Soc. civ. Engrs* **42**, 100 (1955).
[17] D. F. BROOKS and D. M. BROTTON, Computer systems for analysis of large frameworks. *Proc. Am. Soc. civ. Engrs* **93**, 1–23 (1967).
[18] J. H. ARGYRIS, Continua and Discontinua, *Proc. Conf. on Matrix Methods in Structural Mechanics.* Air Force Inst. of Tech., Wright Patterson A.F.B. (1965).
[19] F. B. HILDERBRAND, *Introduction to Numerical Analysis.* McGraw-Hill (1956).
[20] S. LEVY, Square plate with clamped edges under normal pressure producing large deflections, NACA TN. 847 (1942).
[21] K. MARGUERRE, The apparent width of a plate in compression–NACA TM. 833 (1937).
[22] O. C. ZIENKIEWICZ, *The Finite Element Method in Structural and Continuum Mechanics.* McGraw-Hill, 1967.

APPENDIX 1

Stiffness matrix for shell element

The derivation of the incremental stiffness for a shallow shell element shown in Fig. 14 follows that for the curved beam element.

The nodes are denoted by i, j, k, l and displacements in the x, y, z directions by u, v, w respectively. The degrees of freedom at node i are w_i, θ_{xi}, θ_{yi}, u_i and v_i ($\theta_{xi} \equiv \partial w / \partial x'_i$).

For initial deflection w_0 and final deflections w, u, v the strain energy of the element is

$$U = \frac{D}{2}\int_0^b \int_0^a [(w_{xx} - w_{0,xx} + \nu w_{yy} - \nu w_{0,yy})(w_{xx} - w_{0,xx})$$
$$+ (w_{yy} - w_{0,yy} + \nu w_{xx} - \nu w_{0,xx})(w_{yy} - w_{0,yy}) + 2(1-\nu)(w_{xy} - w_{0,xy})^2]\,dx\,dy$$
$$+ B\int_0^b \int_0^a [(u_x + \tfrac{1}{2}w_x^2 - \tfrac{1}{2}w_{0,x}^2)^2 + (v_y + \tfrac{1}{2}w_y^2 - \tfrac{1}{2}w_{0,y}^2)^2$$

$$+2\nu(u_x+\tfrac{1}{2}w_x^2-\tfrac{1}{2}w_{0,x}^2)(v_y+\tfrac{1}{2}w_y^2-\tfrac{1}{2}w_{0,y}^2)$$
$$+\tfrac{1}{2}(1-\nu)(u_y+v_x+w_xw_y-w_{0,x}w_{0,y})^2]\,dx\,dy$$

where $D = Eh^3/12(1-\nu^2)$; $B = Eh/2(1-\nu^2)$. Let Δ denote increments in u, v and w. Then

$$U+\Delta U = \frac{D}{2}\int_0^b\int_0^a[(w_{xx}+\Delta w_{xx}-w_{0,xx}+\nu w_{yy}+\nu\Delta w_{yy}-\nu w_{0,yy})(w_{xx}+\Delta w_{xx}$$
$$-w_{0,xx})+\text{etc.}]\,dx\,dy$$

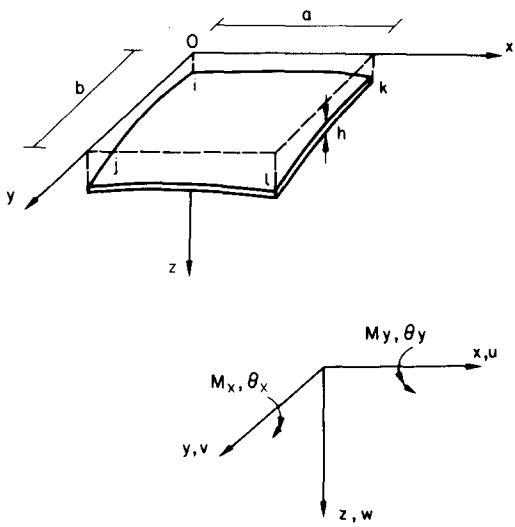

FIG. 14. Shallow shell element.

Substituting ΔU into equation (6), cancelling terms equivalent to P_i and neglecting third and higher order terms in incremental quantities we obtain the matrix form equivalent to equation (8).

$$\{\delta\Delta_q\}^T\{\Delta P\} = \int_0^b\int_0^a \delta[\Delta w_{xx}, \Delta w_{yy}, 2\Delta w_{xy}, \Delta u_x, \Delta u_y, \Delta v_x, \Delta v_y]$$

$$\times\begin{bmatrix} D & \nu D & & & & & \\ \nu D & D & & & & & \\ & & \frac{D(1-\nu)}{2} & & & & \\ & & & 2B & & & 2\nu B \\ & & & & B(1-\nu) & B(1-\nu) & \\ & & & & B(1-\nu) & B(1-\nu) & \\ & & & 2\nu B & & & 2B \end{bmatrix}\begin{bmatrix} \Delta w_{xx} \\ \Delta w_{yy} \\ 2\Delta w_{xy} \\ \Delta u_x \\ \Delta u_y \\ \Delta v_x \\ \Delta v_y \end{bmatrix} dx\,dy$$

$$+\int_0^b\int_0^a \delta[\Delta w_x, \Delta w_y, \Delta u_x, \Delta u_y, \Delta v_x, \Delta v_y]$$

$$\begin{bmatrix}
2Bu_x + 2vBv_y & B(1-v) \times \{u_y + v_x\} & & & & & \\
3Bw_x^2 + Bw_y^2 & 2Bw_x w_y & 2Bw_x & B(1-v) \times w_y & B(1-v) \times w_y & 2vB \times w_x & \Delta w_x \\
-B(w_{0,x}^2 + vw_{0,y}^2) & -B(1-v) \times w_{0,x} w_{0,y} & & & & & \\
\hline
B(1-v) \times \{u_y + v_x\} & 2Bv_y + 2vBu_x & & & & & \\
2Bw_x w_y & 3Bw_y^2 + Bw_x^2 & 2vB \times w_y & B(1-v) \times w_x & B(1-v) \times w_x & 2Bw_y & \Delta w_y \\
-B(1-v) \times w_{0,x} w_{0,y} & -B(w_{0,y}^2 + vw_{0,x}^2) & & & & & \\
\hline
2Bw_x & 2vBw_y & & & & & \Delta u_x \\
\hline
B(1-v)w_y & B(1-v)w_x & & & & & \Delta u_y \\
\hline
B(1-v)w_y & B(1-v)w_x & & & & & \Delta v_x \\
\hline
2vBw_x & 2Bw_y & & & & & \Delta v_y
\end{bmatrix} \mathrm{d}x\,\mathrm{d}y.$$

The displacement functions chosen for w, u and v are as follows:

$$w = [1, x, y, x^2, xy, y^2, x^3, x^2y, xy^2, y^3, x^3y, xy^3, 0, 0, 0, 0, 0, 0, 0, 0]\{\alpha\}$$

$$u = [0, 0, \ldots \text{etc.} \qquad 1, x, y, xy, 0, 0, 0, 0]\{\alpha\}$$

$$v = [0, 0, \ldots \text{etc.} \qquad 0, 0, 0, 0, 1, x, y, xy]\{\alpha\}.$$

Proceedings as for equations (8)–(13) we again obtain the form

$$\Delta P = [K_{\text{lin}} + K_G]\{\Delta q\}$$

The formation of $[K_G]$ will involve the following integral

$$\int_0^b \int_0^a [S_2^p]^T [K_2^p][S_2^p]\,\mathrm{d}x\,\mathrm{d}y \tag{1a}$$

which is similar to equation (13), the p's implying for a plate. The multiplication of the above matrices leads to a (20, 20) matrix, a typical element of which might be

$$x^3y^3\{2Bv_y + 2vBu_x + 3Bw_y{}^2 + Bw_x^2 - B(w_{0,y}^2 + vw_{0,x}^2)\}.$$

Consideration of the shape functions will indicate that the obtaining of the explicit form of the double integral equation (1a) is indeed a formidable task. Hence in the present work, the integration was performed numerically in the computer, using the Gaussian quadrature formulae (Zienkiewicz [22]).

APPENDIX 2

Newton–Raphson method

The Newton–Raphson method [19] has been used [2, 3] and in conjunction with a perturbation technique [4] to solve the sets of nonlinear equations derived from equation (1). It is here shown that the Jacobian matrix used in that method is identical with the linear incremental stiffness matrix.

Consider the solution of two nonlinear, algebraic, simultaneous equations in variables q_1, q_2

$$f(q_1, q_2) = 0$$

$$g(q_1, q_2) = 0$$

and let α_1, α_2 be roots of these equations. Expanding f, g as Taylor series in the neighbourhood of α_1, α_2

$$f(\alpha_1, \alpha_2) = 0 \simeq f(q_1, q_2) + (\alpha_1 - q_1)\left(\frac{\partial f}{\partial q_1}\right)_{q_1, q_2} + (\alpha_2 - q_2)\left(\frac{\partial f}{\partial q_2}\right)_{q_1, q_2}$$

$$g(\alpha_1, \alpha_2) = 0 \simeq g(q_1, q_2) + (\alpha_1 - q_1)\left(\frac{\partial g}{\partial q_1}\right)_{q_1, q_2} + (\alpha_2 - q_2)\left(\frac{\partial g}{\partial q_2}\right)_{q_1, q_2}.$$

Thus

$$\Delta q_1 \frac{\partial f}{\partial q_1} + \Delta q_2 \frac{\partial f}{\partial q_2} = -f$$

$$\Delta q_1 \frac{\partial g}{\partial q_1} + \Delta q_2 \frac{\partial g}{\partial q_2} = -g$$

where $\Delta q_1 \simeq \alpha_1 - q_1$, $\Delta q_2 \simeq \alpha_2 - q_2$ and the values of f, g and their derivatives are the values at q_1, q_2. Hence the following recurrence formula can be constructed.

$$\begin{bmatrix} \frac{\partial f}{\partial q_1}, & \frac{\partial f}{\partial q_2} \\ \frac{\partial g}{\partial q_1}, & \frac{\partial g}{\partial q_2} \end{bmatrix}_K \begin{bmatrix} \Delta q_1 \\ \Delta q_2 \end{bmatrix}_{K+1} = -\begin{bmatrix} f \\ g \end{bmatrix}_K \tag{1b}$$

i.e.

$$[J]_K \{\Delta q\}_{K+1} = -\{F\}_K.$$

Equation (1b) is true for any number of variables q_i and

$$[J] = \frac{\partial(f, g, \ldots)}{\partial(q_1, q_2 \ldots)}$$

is the Jacobian of $f, g, \ldots$.

Now return to equation (1). The force displacement equations derived from this equation can be written

$$\frac{\partial U}{\partial q_1} - P_1 = 0 = f(q_1, q_2 \ldots)$$
$$\frac{\partial U}{\partial q_2} - P_2 = 0 = g(q_1, q_2 \ldots) \tag{2b}$$

If the Newton–Raphson method is applied keeping loads P_i constant

$$[J] \equiv \begin{bmatrix} \dfrac{\partial^2 U}{\partial q_1^2}, \dfrac{\partial^2 U}{\partial q_1, \partial q_2} \cdots \\ \dfrac{\partial^2 U}{\partial q_2 \partial q_1} \\ \vdots \end{bmatrix} \tag{3b}$$

Differentiation of equation (1) with respect to q_j yields

$$\frac{\partial^2 U}{\partial q_i, \partial q_j} = \frac{\partial P_i}{\partial q_j} \simeq \frac{\Delta P_i}{\Delta q_j}$$
$$\frac{\partial^2 U}{\partial q_i \partial q_j} . \Delta q_j \simeq \Delta P_i .$$

The stiffness coefficient relating the increase in nodal force ΔP_i to the increase in nodal displacement Δq_j is

$$\frac{\partial^2 U}{\partial q_i \partial q_j} = K_{\text{inc } ij}$$

Then from equation (3b) we have

$$K_{\text{inc } ij} = J_{ij} \tag{4b}$$

i.e. the Jacobian matrix for displacements $\{q\}_k$ is identical to the linear incremental stiffness matrix for displacements $\{q\}K$.

Slight modification of the preceding theory is necessary when Newton–Raphson iteration is performed keeping one of the displacements constant instead of the loads.

(*Received* 18 *September* 1970)

Абстракт—Указывается достоинство использования линеаризованой матрицы коэффициентов жескикости для среднего приращения в анализе приращения конечного элемента, для нелинейных структур. Метод применяется для закритического анализа несовершенного прямого стержня и пластинки. Особенностью этой работы является ясное представление процесса приращения, использование теории пологих оболочек Маргерра с целью избежения преобразований между локальными и глобальными осями и расчет напряжений в закритическом состоянии. Указывается рподобие расчета для процессов приращения и имеративного Ньютона-Рафсона.